Electroreduction of nitrate ion on Pt, Ir and on 70:30 Pt:Ir alloy

Soledad Ureta-Zañartu and Claudia Yáñez

Departamento de Ciencias Químicas, Facultad de Química y Biología, Universidad de Santiago de Chile, Casilla 40, Santiago 33, Chile

Abstract—The electro-reduction of nitrate ions in acid medium on Pt, Ir and on a 70:30 Pt:Ir alloy was studied by cyclic voltammetry. The alloy has a higher activity than the pure metals, which was interpreted as being due to bifunctional catalysis. Values for activation energies evaluated from the experimental data and Arrhenius plot are discussed.

INTRODUCTION

A number of basic electrochemical research works related to nitrate ion reduction have been reported in the last two decades [1, 2]. The electrochemistry of this compound is a matter of importance in cleaning and monitoring nitrogen oxides in air and water, and also the removal of nitrates from concentrated acid in solutions of radioactive elements [3]. Most of the work has been carried out in aqueous solutions at room temperature, but also in molten salts [4]. The role of nitrite ions and the nature of the reduction products remain unsolved, since nitrate ion reduction is very complex, involving different mechanisms with a large number of stable intermediates [5].

Substantial efforts have been made to design active, selective electrodes. Single crystals [6], water-soluble porphyrins [7] and other modified electrodes [8, 9], and conductive polymers [10] have been extensively studied. However, little has been done with alloys of noble metals. It is well known that adsorption of a metal (*eg* by UPD) on a bare electode, can modify its activity [11]. It is important to find electrodes active for reduction of N_xO_y species to non-toxic compounds or to useful chemicals like hydroxylamine and ammonia. Interesting results have been obtained with Pt—Pd [12] and Pt—Ir [13] for ethylene glycol electro-oxidation and with Pt—Ir alloys for the electroreduction of H_2O_2 [14].

We have carried out a detailed study of the electrochemical reduction of nitrate ions on Pt, Ir and a 70:30 Pt:Ir alloy in order to determine the effect of the electrode material, the electrolyte and temperature, on the reduction rate of nitrate ion.

EXPERIMENTAL

Cyclic voltammetry (*cv*) and gas chromatography (GC) were the main experimental methods. Electrochemical measurements were carried out in a glass cell provided with a water jacket for temperature control. The cell had two compartments (work and counter electrode) separated by a wet conical glass stopcock, and electrical contact was achieved through the thin liquid electrolyte film in the cone. Pt and Ir wire, 0.5 mm in diameter and 99.99% pure, were from Aldrich, as well as a wire of a 70–30 Pt—Ir alloy were used as work electrode and platinum helix was the counter. The reference electrode, a saturated calomel electrode (*sce*), was connected *via* a Luggin capillary. The reference electrode was non-isothermal, *ie*, its temperature was kept constant while that of the working electrode was changed as desired. There must be a temperature gradient somewhere along the Luggin capillary, causing a small thermal junction potential [15].

Merck p.a. $HClO_4$, H_2SO_4 and $NaNO_3$ were used. The water was deionized and twice distilled. Before each experiment the solutions were deaerated by nitrogen bubbling, and a nitrogen stream was maintained over the solution during the measurements. Argon was used for deaerating in GC.

Before each measurement the working electrode was cycled between -0.23 and 1.3 V at 0.1 V/s until the typical *cv* for a clean electrode was obtained. The surface area was estimated from the hydrogen charge, assuming 217 μC cm^{-2} for a monolayer of adsorbed hydrogen on iridium [16] and 224 μC cm^{-2} on

platinum [17]. The electrochemical equipment has been described elsewhere [18].

Polarization curves were recorded at 1 mV/s at different temperatures. In separate experiments, reduction under continuous stirring by argon bubbling of a given amount of sodium nitrate was studied. The gaseous samples were immediately analyzed by GC. Chromatograms were recorded with a Perkin-Elmer 8500p instrument provided with thermal conductivity detector and a Porapak Q column.

RESULTS AND DISCUSSION

Platinum electrode

Figure 1 shows *cv* curves obtained in 0.5 M $HClO_4$ (Fig. 1(A)), 14:1 [v/v] 0.5 M $HClO_4$:0.5 M H_2SO_4 (Fig. 1(B)) and 0.5 M H_2SO_4 (Fig. 1(C)), without (dashed lines) and with (solid lines) 0.1 M $NaNO_3$. The scans were started at the positive limit, and involved the double layer and hydrogen regions. The typical *cv* for the Pt electrode in 0.5 M $HClO_4$ (Fig. 1(A)) changes in the presence of nitrate (solid line), only one peak (peak I) of nitrate reduction being observed in the negative scan, while a new reduction peak (peak II) appears in the positive scan, due to nitrate reduction on the "fresh" surface sites produced by hydrogen desorption. Addition of H_2SO_4 to the $HClO_4$ supporting electrolyte at the same sodium nitrate concentration decreases the reduction rate, producing a significant change in the shape of the *cv* probably due to adsorption competition between sulfate and nitrate anions [19]. When the experiment is carried out in the presence of nitrate in 0.5 M H_2SO_4 (Fig. 1(C)), both processes, reduction of nitrates and hydrogen adsorption, are inhibited. The upper potential limit was +0.3 V (*sce*) in order to avoid poisoning of the Pt. The negative limit was −0.23 V, to avoid H_2 evolution. The reduction of nitrate starts in the double-layer region and is characterized by a current maximum at around −0.15 V for both directions of the scan. However, it must be kept in mind that the current is the sum of two processes, the reduction of nitrate ions and the hydrogen adsorption–desorption. The *cv* in the region between −0.1 V to +0.3 V is unaffected by stirring, suggesting that the process is under adsorption control. M. Sánchez-Cruz *et al.* [20] working in 1 N $HClO_4$ with iridium electrodes that had a hydrous oxide layer growth, detected chloride by ion selective electrode in large quantities after electrolysis, which was explained through an electrochemical reduction to adsorbed chloride, *ie*

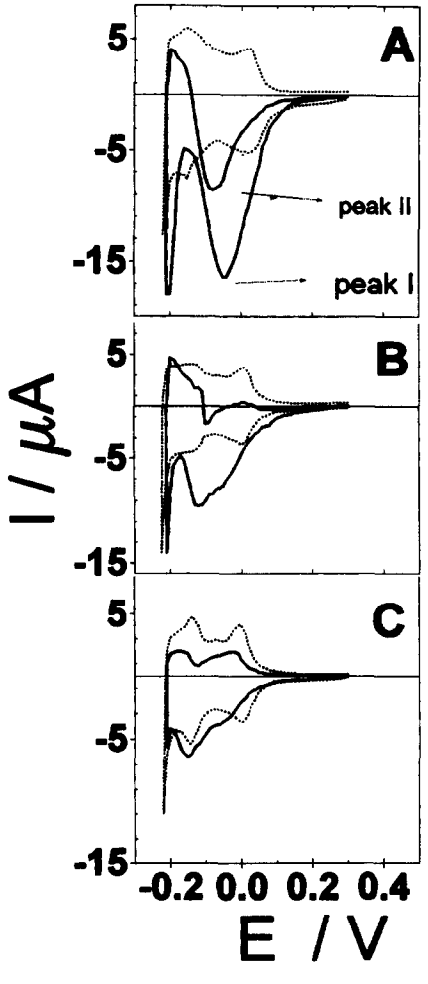

Fig. 1. Cyclic voltammograms at 5 mV/s of a Pt electrode in: (A) 0.5 M $HClO_4$; (B) 14:1 [v/v] 0.5 M $HClO_4$:0.5 M H_2SO_4; and (C) 0.5 M H_2SO_4, without (---) and with (——) 0.1 M $NaNO_3$.

$$ClO_4^- + 8H_3O^+ + 8e \rightarrow Cl^- + 8H_2O. \quad (1)$$

Therefore, when perchlorate ions are reduced on the electrode surface, a change in the I/E profile must be observed as a consequence of Cl^- ions. There would then have to be observed a decrease in the reaction rate.

Studies carried out in our laboratory with chloride ions in the electrolyte, showed that these ions have a meaningful influence on the *cv* of Pt electrode. This influence is greater in the hydrogen adsorption/desorption potential regions. These results demonstrate that adsorbed chloride inhibits the hydrogen adsorption more than nitrate reduction. These studies showed that in our experimental conditions:

(i) The cathodic peak (peak I) was observed in the absence of ClO_4^- anions.

(ii) The current density of this peak is independent of $[ClO_4^-]$ and dependent on $[NO_3^-]$.

(iii) In the absence of nitrate, current density of cathodic currents tends to decrease when chloride ions are added to the electrolyte in a very low quantity.

(iv) Chloride ions were not detected in the electrolyte after exhaustive electrolysis.

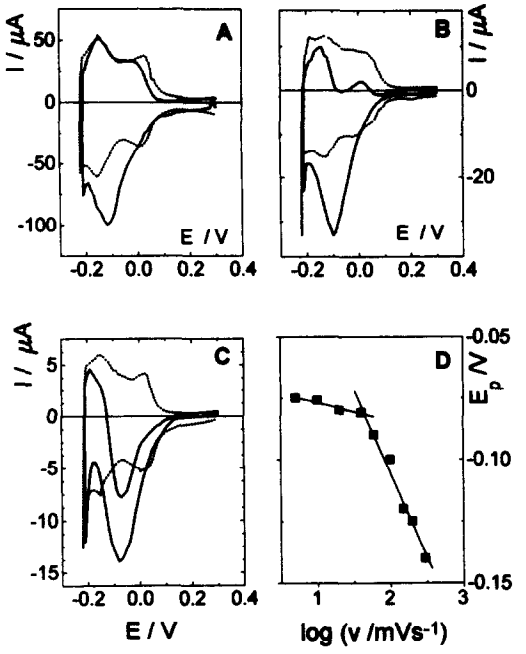

Fig. 2. Cyclic voltammograms of a Pt electrode in 0.5 M $HClO_4$ without (----) and with (——) 0.1 M $NaNO_3$ at the following sweep speeds: (A) 100 mV/s; (B) 10 mV/s and (C) 5 mV/s. A plot of E_p *vs* log v is shown in (D).

The pH dependence has been investigated in the range 0 to 4.5. The ionic strength was maintained with $HClO_4$ and $NaClO_4$ solutions. It was not studied to higher pH values to avoid the introduction of a buffer in the electrolyte. The reduction of nitrate is pH-dependent in the pH range 0–3, in which the electroreduction current decreases with increasing pH. These results are in agreement with those of Petrii *et al.* [5], who found that the passivation region at low potentials corresponds to a high hydrogen coverage.

In Fig. 2 *cv*s at different scan rates, with and without nitrate, are shown. The nitrate reduction predominates over hydrogen adsorption at low sweep rates. The nitrate peak potential for peak I, E_p, increases linearly towards less negative potentials with decreasing scan rate (Fig. 2(D)), with a break at 50 mV/s. This increase of E_p means that either the reduction of nitrate ions is very slow, so a longer time is needed for the process to occur or, the reaction proceeds on surface sites whose regeneration is the rate-determining step. This regeneration can be by desorption of nitrogenous species or can need the formation of activated superficial sites. The second possibility is more probable, since the current is unaffected by stirring, *ie* is under kinetic control [5] and in the reverse scan (to positive potential) the current again is cathodic. Consequently, the voltammetric parameters were measured at 5 mV/s, in order to evaluate mainly the nitrate ion reduction. This is particularly important at low nitrate concentrations, where the experimental error can be higher.

cv at 5 mV/s for the Pt electrode in 0.5 M $HClO_4 + X$ $NaNO_3$ solution are shown in Fig. 3(A)–(C). The reduction of nitrate already starts in the double-layer region and produces a cathodic peak in the negative scan (see above), which position shifts towards more negative potentials with increasing nitrate concentration (Fig. 3(D)). In the reverse (positive) scan another cathodic peak appears at high nitrate concentrations. The reaction is first-order in nitrate at low concentrations, but changes to zero-order at higher concentrations (Fig. 3(E)). Since nitrate reduction overlaps the hydrogen adsorption–desorption range, a quantitative study is possible only at low scan rates, at which the two reactions can be separated.

Although the shape of the *cv* at 5 mV/s changes with temperature the peak potential of nitrate reduction in *cv* at 5 mV/s is almost constant between 2° and 40°C, but the peak current increased with temperature.

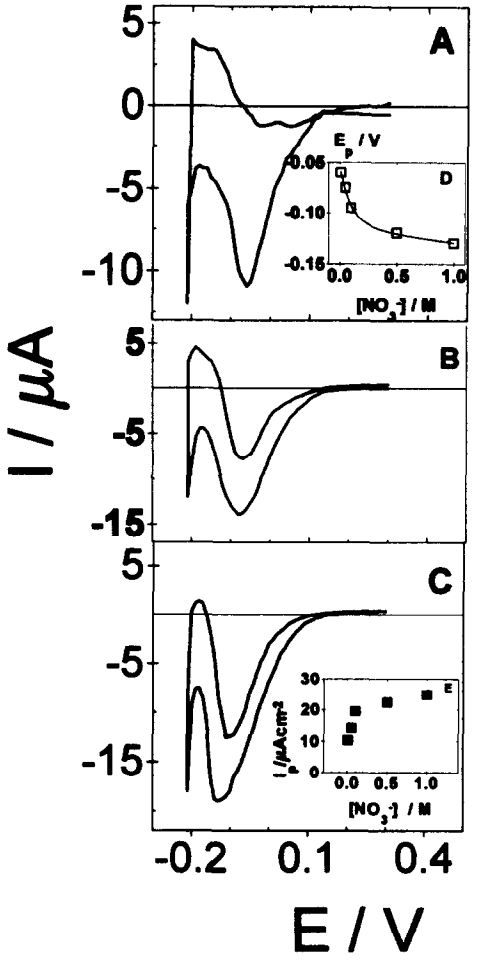

Fig. 3. Effect of the concentration of nitrate ion on the *cv*, at 5 mV/s for a Pt electrode in 0.5 M $HClO_4 + x$ $NaNO_3$ for the following nitrate concentrations x: (A) 0.01 M; (B) 0.1 M; and (C) 1 M in $NaNO_3$. (D) Plot of E_p *vs* $[NO_3^-]$; (E) plot of I_p *vs* $[NO_3^-]$.

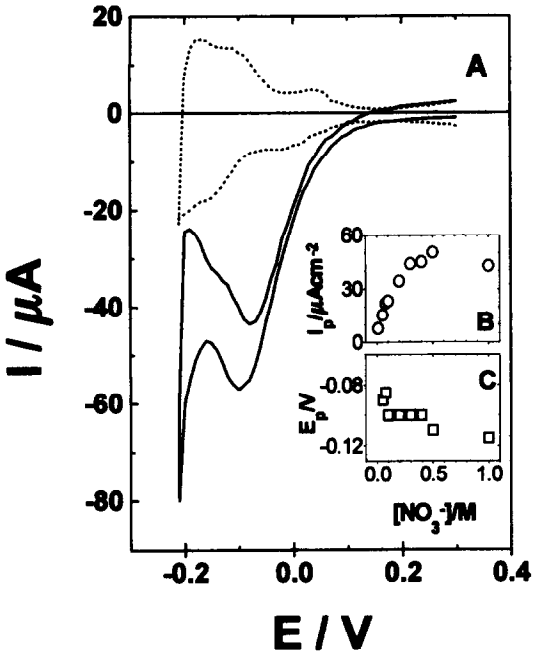

Fig. 4. (A) Cyclic voltammograms at 5 mV/s of an Ir electrode in 0.5 M $HClO_4$ without (---) and with (——) 0.1 M $NaNO_3$. (B) Plot of peak current (I_p) *vs* [NO_3^-] and (C) Plot of peak potential (E_p) *vs* [NO_3^-].

Iridium electrode

On Ir, the onset of nitrate reduction requires less negative potentials than on Pt (Fig. 4(A)). The *cv* changes with the nitrate concentration. It is important that at high nitrate concentrations and low sweep rates the negative and positive scans almost overlap. The reaction order for nitrate is one at low concentrations and zero at higher concentrations (Fig. 4(B)), as with Pt. The peak potential shifts to slightly less positive values as the nitrate concentration increases (Fig. 4(C)). The existence of a limiting current can be explained either by surface saturation with an adsorbed intermediate that poisons the electrode surface, or by control by the rate of regeneration of the active sites.

The *cv*s at 5 mV/s at different temperatures were similar to those obtained with Pt. At high temperatures the negative and positive scans almost coincide. It is possible that the poison on the Ir surface is less strongly bonded than on Pt, *ie* that it desorbs more easily. With iridium, E_p is almost independent of temperature. Tafel slopes near 0.12 V, dependent on temperature, were obtained. This point will be discussed below for all the electrodes.

70:30 Pt:Ir alloy electrode

The *cv*s for the 70–30 Pt—Ir alloy in 0.5 M $HClO_4$ is similar to that for the Pt electrode. Also the *cv*s in 0.5 M $HClO_4$ + 0.1 M $NaNO_3$ are similar to those of Pt and Ir (Fig. 5(A)). The E_p of nitrate reduction decreases towards more negative potentials with increasing nitrate concentration (Fig. 5(B)). There is a very small range of nitrate concentrations over which the reaction is first-order (Fig. 5(C)). The shape of the *cv* changes with temperature, as with Pt, and a very important increase of the peak current with temperature is observed.

Gas chromatographic analysis

Gas chromatographic analyses were carried out by repetitive cyclic voltammetry with stirring by bubbling of the electrolyte using a Pt black electrode of high area and a long electrolysis time. (It was not possible to use a Pt—Ir electrode of high real area.) The analysis detected only traces of N_2O, with poor reproducibility. No N_2 could be detected. Several authors [21, 22] have previously established that the N_2O obtained in nitrate ion reduction on Pt in acidic solution reacts with adsorbed hydrogen fast and irreversibly, regenerating the Pt site for new hydrogen adsorption. This can be the reason why it was not possible to obtain reproducible measurements of N_2O by GC. These results are in good agreement with those of Enyo *et al.* [23] on a Pt electrode with on-line mass spectroscopy for the electroreduction of nitrite and nitrate ions in sulfate solutions. They detected species with m/e-values of 28 and 44, corresponding to $^{14}N^{14}N^+$ and $^{14}N^{14}N^{16}O^+$, respectively, at potentials in the hydrogen region, and at higher potentials a species with $m/e = 30$, corresponding to the $^{14}N^{16}O^+$ ion.

DISCUSSION

At low nitrate concentrations, nitrate reduction is a first order process for the three electrodes. At higher

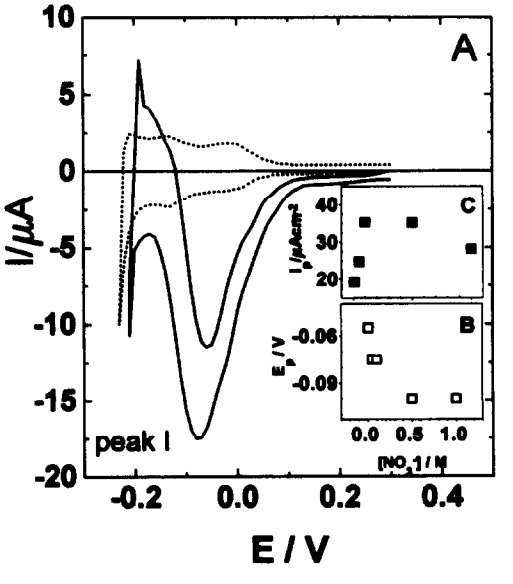

Fig. 5. (A) Cyclic voltammograms at 5 mV/s of a 70:30 Pt—Ir electrode in 0.5 M $HClO_4$ without (——) and with (——) 0.1 M $NaNO_3$. (B) Plot of E_p *vs* [NO_3^-]; and (C) Plot of I_p *vs* [NO_3^-].

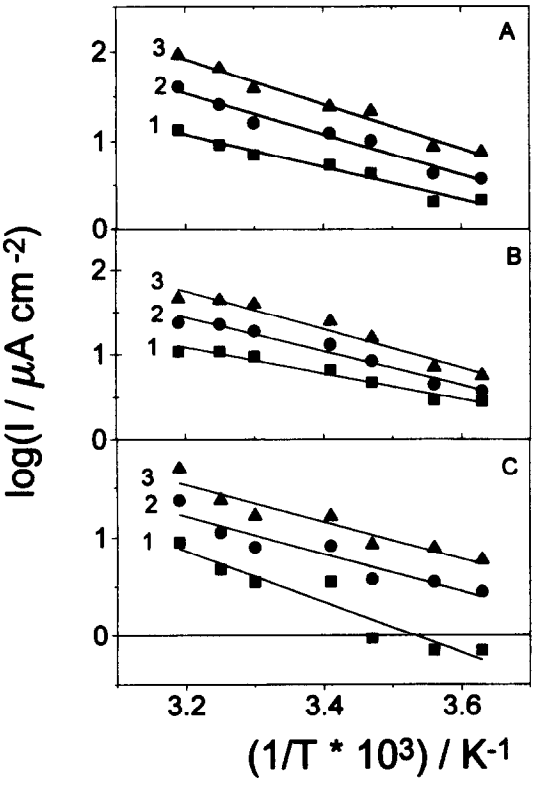

Fig. 6. Arrhenius plot obtained from polarization curves at 1 mV/s in 0.5 M $HClO_4$ + 0.1 M $NaNO_3$ for the following potential: (1) $E = -0.1$ V; (2) $E = -0.05$ V; and (3) $E = 0.0$ V *vs* (*sce*) for (A) Pt; (B) Ir; and (C) 70:30 Pt:Ir alloy.

nitrate concentrations the order is zero (limiting current), probably due to blocking of surface sites, suggesting that the reaction is controlled by regeneration of specific sites.

The different behavior observed for the three electrodes is probably a consequence of differences in the nitrate ion interaction with each electrodic surface. It is known that already at 0.3/V *vs rhe* (initial potential in the *cv*) Ir develops an oxy-hydroxy-hydrated surface oxide which is resistant to reduction [24]. Reduction of this oxide in the hydrogen region creates active surface sites on which adsorption and subsequent reduction of the nitrate ions occur more easily.

The slopes of Tafel plots in 0.5 M $HClO_4$ + 0.1 M $NaNO_3$ obtained from sweeps at 1 mV s depended on temperature. When an electrochemical reaction occurs in several stages, the Tafel slope ($b = \{\partial\eta/\partial \log I\}_E$) reflects the steps up to, and including that limiting the rate. With adsorbed intermediates the activation is not an Arrhenius process. When b is independent of T, there should be an approximately linear dependency of the experimental transfer coefficient α, on temperature, $b = RT/\alpha(T)F$ [25]. However, if the reaction mechanism is catalytic, the preferred hypothesis is that in the heterogeneous catalytic process the apparent activation energy changes linearly with the logarithm of the pre-exponential factor of the Arrhenius equation according to [26]:

$$\ln A = B + e\Delta H^{\neq}, \tag{2}$$

where A is the frequency factor and $\Delta H^{\neq}$ the activation energy of the Arrhenius equation, and B and e are constants characteristic of a group of reactions that show this compensation effect. The constant "e" is normally positive, and so the pre-exponential term increases with the activation energy. Equation (1) leads to [26]:

$$\ln k = B + \Delta H^{\neq}\left(e - \frac{1}{RT}\right), \tag{3}$$

which shows that there is a temperature, the "isokinetic temperature" ($\beta = 1/\{eR\}$). Value of the rate constant "k" at the "isokinetic temperature" is known as the isokinetic constant.

An Arrhenius plot of the polarization curves is shown in Fig. 6. A linear behavior obtains, but the lines at different potentials have different slopes, which is not surprising for systems where the state of the electrode surface depends on the potential. Table 1 shows the results obtained from Fig. 6.

The Pt—Ir electrode has the lowest $\Delta H^{\neq}$ at 0.0 V and -0.05 V, and the highest value at -0.1 V. While for Pt—Ir $\Delta H^{\neq}$ decreases as the potential increases, Pt and Ir show the opposite behavior from the E and ln$A$ values in Table 1 The isokinetic temperatures are -50°C for Pt, -25°C for Ir and 131°C for the Pt—Ir alloy, *ie* the temperature range used (2°–35°C) was higher than the isokinetic temperatures for Pt and Ir, and lower for Pt—Ir, as readily observed in Fig. 6. For the three electrodes the potential with the lowest $\Delta H^{\neq}$ is $E = 0.0$ V (*sce*) (see line 3 in Fig. 6). However, for Ir and Pt (Fig. 6(A) and (B)) line 3

Table 1.
Values of $\Delta H^{\neq}$ and ln A obtained from the Arrhenius plots in Fig. 6

	$\Delta H^{\neq}$ (kJ mol)			ln A		
Electrode	$E = -0.1$ V	$E = -0.05$ V	$E = 0.0$ V	$E = -0.1$ V	$E = -0.05$ V	$E = 0.0$ V
Pt	35.3	43.7	47.5	16.1	20.3	22.7
Ir	29.1	37.9	43.3	13.7	17.9	20.7
Pt–Ir 70:30	49.4	36.2	35.6	21.1	16.8	17.2

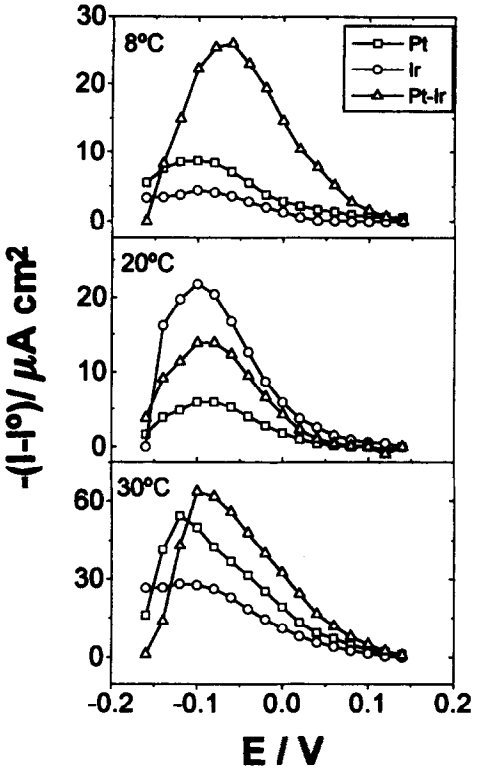

Fig. 7. Normalized *cv* at 5 mV/s of $-(I - I^0)$ *vs E*. I and I^0 are the currents in the negative scan in 0.5 M $HClO_4$ with and without 0.1 M $NaNO_3$, respectively. (A) 8°C; (B) 20°C; and (C) 30°C.

shows ΔH^* values higher than lines 1 and 2 for the same electrode, while for Pt—Ir line 3 has the lowest ΔH^* value. The results for the Pt—Ir electrode can be due to variations of the properties of the surface oxide film, presumably dependent on temperature and adsorption of the intermediates and anions of the electrolyte. Furthermore, the surface coverage is a function of potential and temperature.

In order to compare the electrocatalytic activities of the three electrodes, *cvs* at 5 mV/s were normalized by plotting $I - I^0$ *vs E*, I and I^0 being the currents obtained in the scan towards negative potentials, in the presence and absence of 0.1 M $NaNO_3$, respectiely. Plots corresponding to three different temperatures are shown in Fig. 7. It is clear that at 8° and 20°C the Pt and Ir electrodes are poor catalysts with an activity maximum near −0.1 V, while the Pt—Ir alloy has a higher activity over a wide range of potentials (Fig. 7(A) and (B)). However, at 30°C the Ir electrode has the highest activity (Fig. 7(C)). The three electrodes show a higher activity at 30°C than at 8 and 20°C, especially the iridium electrode. The activity in *cvs* at 5 mV/s is different from that in scans at 1 mV/s, especially at 30°C, as was to be expected for electrodes whose activity completely depends on their history.

The observed kinetics of nitrate ion reduction can be modelled in terms of bifunctional catalysis, the Pt sites acting as adsorption sites, and the Ir sites nucleating oxygen containing species at potentials 0.2–0.3 V less than on Pt.

Vetter [27] proposed a reaction sequence in which electroreduction is undergone, not by the NO_3^- ion itself, but by NO_2 formed in a preceding reaction or to be added to the electrolyte as a catalyst. With our results, we propose a reaction sequence that can be written as the following cyclic process:

$$\begin{array}{ccc} 2HNO_2 & \longrightarrow & 2NO^+ + 2H_2O \\ \uparrow & & \downarrow \\ 2H^+ + 2e & & NO_3^- \\ \downarrow & & \downarrow \\ 2NO_2 & \longleftarrow & N_2O_4 \longrightarrow N_2O + 3/2O_2 \end{array} \qquad (4)$$

in which the NO_2 or HNO_2 molecules are produced in an initial step of adsorption of nitrate ions, as proposed by Horanyi *et al.* [19] for the electroreduction of nitric acid on Pt:

$$HNO_3 \rightarrow (HNO_3)_{ad}, \qquad (5)$$

$$(HNO_3)_{ad} + 2H_{ad} \rightarrow HNO_2 + H_2O. \qquad (6)$$

This mechanism is consistent with the reaction order (one at low nitrate concentrations and zero at higher concentrations), and also with the observed decrease of the reduction rate with increasing pH. The rate determining step must be reaction (6), which needs two H_{ad} for one H_2O molecule, this being the main origin of the difference in the catalytic activity of the three electrodes. As the Ir electrode adsorbs OH at lower potentials than Pt, it is likely that instead of reaction (5) the following reactions occur:

$$2Ir + 2H_2O \rightarrow 2Ir—OH + 2H^+ + 2e$$

$$(HNO_3)_{ads} + 2H^+ + 2e \rightarrow HNO_2 + H_2O$$

$$2Ir + 2H_2O + (HNO_3)_{ads} \rightarrow 2Ir—OH + N_2O + H_2O. \qquad (7)$$

Tests accomplished adding small quantities of HNO_2 solutions to the electrolyte showed an increase in the cathodic current, highest to wait for the nitrite reaction.

ACKNOWLEDGEMENTS

Financial support from DICYT-USACH and FONDECYT (grants 91-41-uz and 1930093) is gratefully acknowledged. We thank C. Gutiérrez for his comments about the manuscript.

REFERENCES

1. G. Horanyi and E. M. Rizmayer, *J. Electroanal. Chem.* **188**, 265 (1985) and references cited therein.

2. A. J. Calandra, C. Tamayo, J. Herrera and A. J. Arvía, *Electrochim Acta* **17,** 2035 (1972) and references cited therein.
3. S. Sunohara, K. Nishimura, K. Yahikozawa, M. Ueno, M. Enyo and Y. Takasu, *J. Electroanal. Chem.* **354,** 161 (1993).
4. I. B. Singh, S. Sultan and K. Balakrisnan, *Electrochim. Acta* **38,** 2611 (1993).
5. A. A. Petrii and T. Ya. Safonova, *J. Electroanal. Chem.* **331,** 897 (1992).
6. R. Naneva, T. Vitanov, N. Dimitrov, V. Bostanov and A. Popov, *J. Electroanal. Chem.* **328,** 287 (1992).
7. C. H. Yu and Y. O. Su, *J. Electroanal. Chem.* **368,** 323 (1994).
8. F. El Omar and R. Durand, *J. Electroanal. Chem.* **178,** 343 (1984).
9. H. Huang, M. Zhao, X. Xing, I. T. Bae and D. Scherson, *J. Electroanal. Chem.* **293,** 279 (1990).
10. G. Mengoli and M. M. Musiani, *J. Electroanal. Chem.* **269,** 99 (1989).
11. G. Ritzoulis, *J. Electroanal. Chem.* **327,** 209 (1992).
12. N. Dalbay and F. Kadirgan, *Electrochim. Acta* **36,** 353 (1991).
13. M. S. Ureta-Zañartu, C. Yáñez, M. Páez and G. Reyes, *J. Electroanal. Chem.* **405,** 159 (1996).
14. Y. Zhang and G. S. Wilson, *J. Electroanal. Chem.* **345,** 253 (1993).
15. E. Gileadi, *Electrode Kinetics for Chemists, Chemical Engineers, and Material Scientists*, p. 153, VCH Publishers, Inc (1993).
16. M. Watanabe and S. Motoo, *J. Electroanal. Chem.* **202,** 125 (1986).
17. J. O'M Bockris and K. T. Jeng, *J. Electroanal. Chem.* **330,** 541 (1992).
18. M. S. Ureta-Zañartu, P. Bravo and J. H. Zagal, *J. Electroanal. Chem.* **337,** 241 (1992).
19. G. Horányi and E. M. Rizmayer, *J. Electroanal. Chem.* **140,** 347 (1982).
20. M. Sánchez-Cruz, J. González-Tejera and C. Villamañán, *Electrochim. Acta* **30,** 1563 (1985).
21. H. Ebert, R. Parsons, G. Ritzoulis and T. Van der Noot, *J. Electroanal. Chem.* **264,** 181 (1989).
22. A. Ahmadi, E. Bracey, R. Wyn Evans and G. Attard, *J. Electroanal. Chem.* **350,** 297 (1993).
23. K. Nishimura, K. Machida and M. Enyo, *Electrochim. Acta* **36,** 877 (1991).
24. L. D. Burke and D. P. Whelan, *J. Electroanal. Chem.* **162,** 121 (1984).
25. B. E. Conway in *Modern Aspects of Electrochemistry* (Edited by B. E. Conway, R. E. White and J. O'M. Bockris) Vol. 16, Ch. 2. Plenum Press, New York (1984).
26. L. Bouyssieres, C. Fores, J. Poblete and F. J. Gil-Llambías, *Appl. Catal.* **23,** 271 (1986).
27. K. Vetter, *Z. Phys. Chem.* **194,** 284 (1950); *Z. Elektrochem.* **63,** 1189 (1959).